

Per E.M. Siegbahn

O-O bond cleavage and alkane hydroxylation in methane monooxygenase

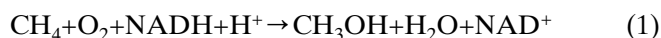
Received: 23 May 2000 / Accepted: 27 September 2000 / Published online: 28 November 2000
© SBIC 2000

Abstract Several new aspects of the O-O bond cleavage and alkane hydroxylation mechanisms have been studied by hybrid density functional theory in this reinvestigation of methane monooxygenase. As concerning key intermediates in these reactions, a new important low-lying state is found, described either as $\text{Fe}_2(\text{III},\text{V})$ or as $\text{Fe}_2(\text{III},\text{IV})\text{O}$. A fully optimized transition state for O-O bond cleavage has been determined. It is suggested that the large difference in optimal size (as determined in gas phase) of the complex, before and after the O-O bond cleavage, leads to an additional driving force for the reaction, not considered previously. The strain of the enzyme is estimated to lead to a driving force in the forward direction of about 5 kcal/mol, which could explain some of the pH dependence found in recent experiments. For the hydroxylation reaction, a clean hydrogen abstraction transition state leading to a substrate radical is again found, in contrast to interpretations of radical clock experiments. An explanation, based on new results, is suggested that could account for both the experimental and theoretical results.

Keywords Methane monooxygenase · O-O bond cleavage · Alkane hydroxylation · Density functional theory

Introduction

Methane monooxygenases (MMOs) are a group of enzymes which convert methane to methanol via a monooxygenase pathway in which the dioxygen molecule is activated [1, 2, 3, 4]. The overall reaction is given by:

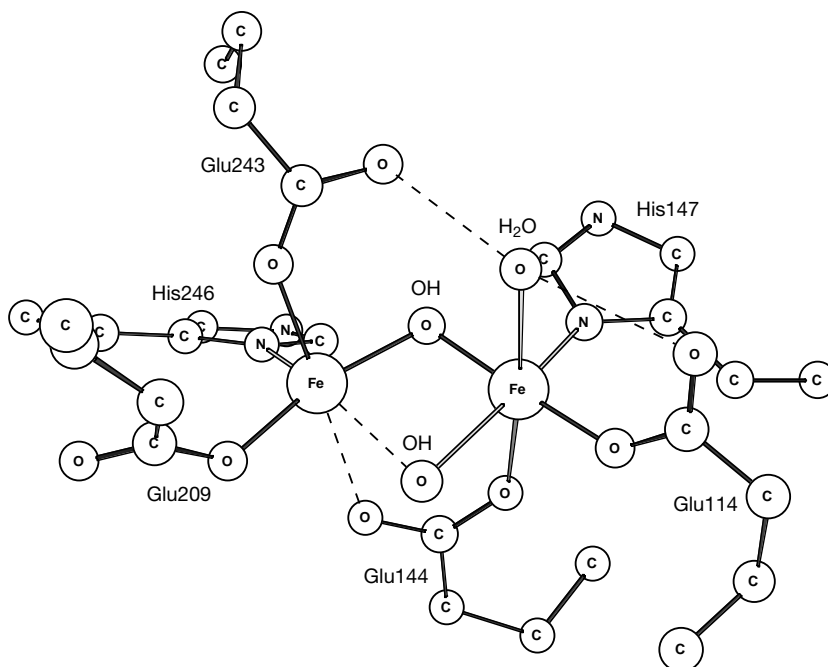


The longest known MMOs are soluble proteins containing a binuclear iron active site. MMOs consist of three proteins, a hydroxylase (MMOH or protein A) containing an iron dimer complex, a reductase (MMOR or protein C), and a regulatory protein (MMOB or protein B). The MMOR component uses NADH as a primary reductant that provides electrons necessary to reduce O_2 , the MMOB component allows MMOH to react rapidly with O_2 to form a peroxide intermediate [5], and the MMOH component interacts with O_2 and carries out the substrate oxidation step. The X-ray structure of MMOH from *Methylococcus capsulatus* (Bath) has been determined both for a diferric complex (see Fig. 1) and for a reduced complex [6, 7]. A structure from *M. trichosporium* for a diferric complex has also been determined [8], and the iron dimer complex was found to be very similar to the one for the other organism. From the known oxidation states of the irons in these complexes, normal charges of carboxylates and histidines, and the assignment of the bridging ligands, the charge of the complexes could be determined as either neutral or possibly +1. In a more recent study of the closely related ribonucleotide reductase R2, the irons were replaced by other metals and also removed, and the charges of the complexes were again found to be nearly neutral (Su X-D, Andersson ME, Rinaldo-Mathis A, Blodig W, Persson BO, Sjöberg B-M, Nordlund P, in preparation), in line with a general rule that metal complexes deeply buried in the low dielectric of a protein should be almost neutral [9, 10, 11, 12].

There have been decades of experimental studies on MMO and several reviews have been written during recent years, where the experimental information obtained so far is covered in detail [1, 2, 3, 4]. Only a few points of special relevance for the present study will be mentioned here. The lowest oxidation state of the diiron complex is $\text{Fe}_2(\text{II},\text{II})$, which is a loosely

P.E.M. Siegbahn (✉)
Department of Physics, Stockholm University, Box 6730,
113 85 Stockholm, Sweden

Fig. 1 X-ray structure of the diferric form of the iron dimer complex of methane monooxygenase from *Methylococcus capsulatus* (Bath)



bound, ferromagnetically coupled dimer with an Fe-Fe distance of 3.4 Å. This complex reacts with O₂ to form another complex P, which is normally assigned to an Fe₂(III,III) peroxide complex. One or more intermediates in this process have been postulated [11]. In the next step, the dioxygen bond is cleaved and an unprecedented Fe₂(IV,IV) complex termed Q is formed. The oxidation state assignment was made based on Mössbauer spectroscopy [13]. Compound Q has been suggested to be the active oxidant that attacks methane. All oxidized intermediates observed in MMO have antiferromagnetic coupling of the iron spins and are therefore EPR invisible when the sum of the oxidation states is even. Compound Q has been studied by EXAFS, based on which an unusual bis- μ -oxo bridged structure was suggested with substantially unequal Fe-O distances of the diamond core and with a very short Fe-Fe distance of only 2.46 Å [14].

The hydroxylation of hydrocarbons by MMO has been studied extensively experimentally and several possible mechanisms have been suggested [1, 2]. These mechanisms fall into essentially two categories: radical and non-radical mechanisms. In the radical mechanisms the first step is hydrogen abstraction from the hydrocarbon, while the non-radical mechanisms suggest a concerted pathway. Support for the hydrogen abstraction mechanism comes from measurements of kinetic isotope effects (KIEs) by Lipscomb and co-workers [2, 15, 16]. For *M. trichosporium*, some of the largest KIEs in biology were observed. Furthermore, radical spin-trap experiments have detected radical species which were able to diffuse out of the protein matrix during the MMO reactions [17]. The results using chiral ethane (CH₃CHDT), giving 35% inversion of configuration, are more difficult to conclusively interpret and have in fact been interpreted in favor of

both the radical mechanism [18] and in favor of a concerted mechanism [19]. Support for a concerted non-radical mechanism of MMO comes mainly from radical clock measurements by Newcomb, Lippard and co-workers [20, 21, 22, 23, 24, 25, 26]. For *M. capsulatus*, very fast radical clocks were studied with results interpreted to show a maximum radical lifetime as short as 10⁻¹⁴ s. Fast radical clocks with *M. trichosporium* MMO gave a small amount of ring opened products, consistent with a somewhat longer radical lifetime of 10⁻¹¹ s [20, 21, 22, 23, 24, 25, 26, 27]. With these short lifetimes, the presence of radicals as intermediates in the hydroxylation was excluded, both for MMO and for the related process of hydroxylation in P-450. In contrast, other recent radical clock experiments have been interpreted in favor of a radical mechanism [28]. Steric strain induced by the protein was used to explain the observed regioselectivity. However, the identification of the product in these methylcubane experiments has been questioned [29]. Instead, the product was suggested to be homocubanol, which is only known to be formed via a cationic process. The discussion of the radical clock experiments will be one of the major topics of the present paper.

Another major topic to be discussed here is O₂ activation by MMO. Both homolytic and heterolytic mechanisms have been suggested [4]. Recently, the effect of solvent pH and deuteration on the transient kinetics of the key intermediates of the dioxygen activation process in *Methylosinus trichosporium* (OB3b) was studied by Lee and Lipscomb [11]. The decay reaction for complex O (the complex that forms after oxygen binds to the protein) was found to be pH independent, while in contrast the P formation rate was found to decrease sharply with increasing pH to near

zero at pH 8.6. The decay rate of P matched the formation rate of Q, and both rates decreased sharply with increasing pH to near zero at pH 8.6. The results were interpreted to suggest that one proton is transferred in both the formation of P and of Q. If these protons are transferred to the bound oxygen molecule, the data are consistent with a model in which water is formed concurrently with the formation of Q, suggesting a heterolytic O-O bond cleavage mechanism similar to the ones suggested to occur in heme oxidases and peroxidases [30, 31, 32].

In recent years, quantum chemical studies have also contributed to the understanding of the mechanism of MMO. In the first density functional theory (DFT) study on MMO (referred to below as paper I), using a quite simple model, structures were suggested for the different intermediates observed [33, 34]. In particular, a structure for compound Q was suggested to have two bridging μ -oxo bonds of different lengths, independently of and simultaneously as the EXAFS study mentioned above. Two of the diamond core distances were 1.8 Å and the other two 2.0 Å. A mechanism for activation of methane by Q was also suggested with a transition state which was one of almost pure hydrogen abstraction leading to a methyl radical. In a more recent study [35] (referred to below as paper II), using a larger model of the iron dimer complex, a quite similar hydrogen abstraction transition state was found. An approximate transition state for O-O bond cleavage using a homolytic mechanism was also determined. In a later study, Basch et al. [36] obtained a quite similar structure for Q and a similar hydrogen abstraction transition state for C-H activation of methane using a smaller model of the iron dimer complex. A new and very interesting aspect in that study is that also a second transition state was found along the hydroxylation path, which occurs for the recombination of the methyl radical with the μ -hydroxo ligand. This step was assumed to occur without a barrier in the previous DFT studies. In a quite recent DFT study, Friesner and co-workers [37] used a very large model containing about 100 atoms as compared to the first DFT study where a model of about 20 atoms were used and the second study where about 40 atoms were used. The impressively large size of the model was found to be necessary in order to obtain a reliable structure for the reduced diferrous complex. This model study also led to a slightly different structure for compound Q, to be discussed further below. In other DFT studies using considerably smaller models, Yoshizawa et al. [38, 39, 40, 41, 42] obtained a concerted insertion pathway for hydroxylation of methane. This mechanism, which is in line with the mechanism suggested by radical clocks but in sharp contrast to the hydrogen abstraction mechanism found in the other studies, was obtained using either charged and unsaturated metal complexes, or a highly excited neutral complex. Shestakov and Shilov [43] have also argued against a radical mechanism and

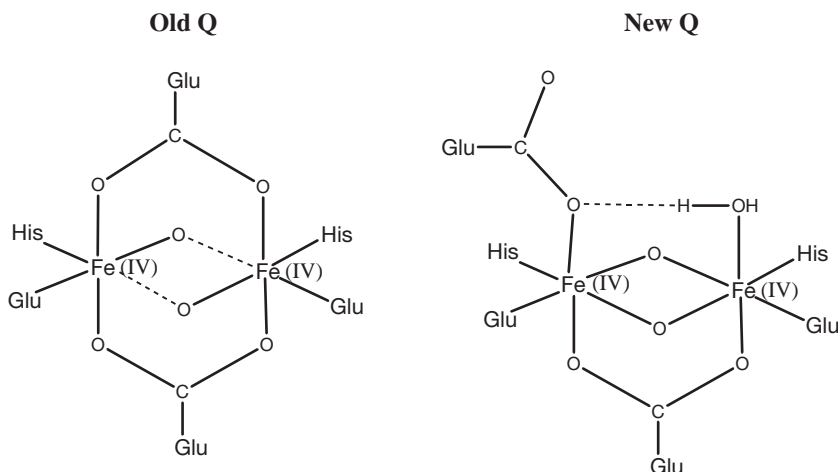
instead suggested a direct insertion involving a five-coordinate carbon intermediate.

In spite of systematic progress in the understanding of the mechanism of MMO, there are still major questions which remain to be answered. The present DFT study will focus on three of these questions. The first one concerns the structure of compound Q, the most oxidized intermediate observed for MMO. The oxidation states were, as mentioned above, first suggested based on Mössbauer spectroscopy to be $\text{Fe}_2(\text{IV},\text{IV})$ and this is now more or less accepted as a correct assignment. After recent EXAFS and theoretical model studies, there is also (to a large extent) consensus that the structure has two bridging μ -oxo bonds, even though a possibility that there is only a single bridging μ -oxo bond cannot be entirely ruled out [44]. With oxidation states of $\text{Fe}_2(\text{IV},\text{IV})$, two bridging oxo groups, two histidines, and four carboxylates, the complex is neutral. In a previous DFT study it was suggested that two of the carboxylates should be bridging, since this led to the best agreement with the unusually short Fe-Fe distance of 2.46 Å obtained by EXAFS. In fact, it is difficult to imagine that any other structure for Q could lead to a shorter Fe-Fe distance. However, based on the recent DFT study by Friesner and co-workers [37], it was suggested that only one of the carboxylates is bridging, and that a water is directly coordinated to one of the iron centers. Of the structures tried, this one led to the lowest energy. This type of structure was never tried in the previous study. The two different structures suggested for compound Q are shown schematically in Fig. 2. The questions addressed here are twofold. First, is the new structure a result of the larger model used in the later study, or is it also the most stable one for the smaller model? Another point addressed in this context is whether the new structure for Q has any implications for the mechanism for O-O bond cleavage or hydroxylation, or if essentially the same mechanisms suggested previously still apply. Comparisons will also be made to recent experimental modeling work on highly oxidized iron dimer complexes [45, 46, 47, 48, 49, 50].

The second major question discussed in the present paper concerns the mechanism of O_2 activation. In the previous study (paper II), only an approximate transition state could be determined [35]. A full optimization will be presented here. In relation to information obtained from these calculations regarding both solvation and temperature effects, the recent results concerning the implications of the measured pH dependence of the reaction [11] will be discussed.

The third main topic discussed here concerns the mechanism for hydroxylation. As mentioned above, the experimental interpretations are in severe conflict with each other and suggest quite different mechanisms. Furthermore, the quite convincing arguments from radical clocks are in striking contrast to the radical mechanisms strongly suggested by theoretical calculations, as described above. It must furthermore be

Fig. 2 Old and new structure suggested for compound Q of MMO



concluded at this stage that a simple solution to this problem, where either the calculations or some of the experiments are wrong, is very unlikely. To analyze this situation further, the chemistry of the radical clocks has been investigated in detail. An explanation that could account for both experimental and theoretical results will be attempted. Efforts in the same direction by Shaik and co-workers for P-450 [51] will be discussed in this context.

Materials and methods

Computational details

The calculations in the present study were done in a similar way as those in the previous studies on MMO [35], and can be divided into three steps. Following an optimization of the geometry using medium-size basis sets, the energy was evaluated using large basis sets. In the third step the effect of the polarized surroundings was evaluated. All these steps were made at the B3LYP level [52, 53, 54, 55] using the Gaussian 94 and 98 programs [56, 57].

In the B3LYP geometry optimizations, standard double-zeta basis sets were employed. For the metal containing systems the LANL2DZ set (from Gaussian 94) was used. This basis set uses an ECP (effective core potential) [58] for the metal atoms. These rather small basis sets can safely be used for the present purposes since it has been clearly shown that the final energy is very insensitive to the quality of the geometry optimization [59, 60]. The B3LYP final energy calculations were made using larger basis sets where the LANL2DZ basis set was extended by adding diffuse functions and a single set of polarization functions for all atoms taken from the 6-311+G(1d,1p) basis set.

The dielectric effects from the surrounding protein were obtained using the self-consistent isodensity polarized continuum model (SCI-PCM) [61, 62]. In this method the cavity is defined self-consistently in terms of a surface of constant charge density for the solute molecule. The default isodensity value of 0.0004 e/B³ was used. The dielectric constant ϵ of the protein is the main empirical parameter of the model and it was chosen to be equal to 4, in line with previous suggestions for proteins. This value corresponds to a dielectric constant of about 3 for the protein itself and of 80 for the water medium surrounding the protein. It should be noted that the present systems are quite insensitive to the choice of ϵ since the charge separations are only minor and for this reason almost negligible dielectric effects were obtained in most cases. In some cases, discussed below, the

cavitation effect is also of interest. The cavitation energy is the energy required to make room in the protein for the molecule being studied, and is related to the surface tension of the protein environment. This effect was evaluated using the polarized continuum models of Tomasi, Barone and co-workers [63, 64, 65, 66].

In contrast to the previous study, where at most only approximate Hessians were calculated, the present calculations include a full determination of a Hessian in each of the important geometry points. This allows for a full account of zero-point vibrational effects and also an estimate of temperature effects. The calculated Hessians are furthermore used to confirm that the equilibrium geometries have essentially no imaginary frequencies and that the transition states have one imaginary frequency. Since very tight convergence is difficult to achieve for the present systems, small imaginary frequencies must also be tolerated, but these are just interpreted as round-off effects and should have no influence on the results. It should finally be added that, for some complexes discussed below, calculations were performed for ferromagnetic coupling of the metal spins even though they are known to be antiferromagnetic. This was done simply because convergence for ferromagnetic coupling is easier to achieve. For the cases where comparisons were made, the energy difference between ferro- and antiferromagnetic couplings is quite small (less than 1 kcal/mol) and within the uncertainty of the present calculations. The choice of spin coupling is therefore extremely unlikely to significantly affect the energetics and thereby the mechanisms discussed below.

Results and discussion

Three different topics will be discussed in this reinvestigation of the mechanism of MMO. The first one concerns a few new aspects of the geometric and electronic structures of possible intermediates of the highly oxidized dimer complex. Under the second topic, implications from a full transition state optimization of the activation of O₂ are described. In particular, some surprising results for the temperature dependence of the reaction are discussed in relation to new results for the protein environment effects. Finally, under the third topic, the mechanism for hydroxylation is discussed in an attempt to rationalize the apparently conflicting results from radical clocks on the one hand, and from kinetic isotope measurements and theoretical calculations on the other hand.

Low-lying states of the dimer complex

Before the new results of the present study are discussed, a short summary of the results obtained in the previous studies is needed. In the first B3LYP study of MMO (paper I) [33], a quite simplified model of the iron dimer complex was used containing 20–25 atoms. Apart from a bridging carboxylate, only hydroxyls and waters were used as models for the actual ligands. Still, a suggested structure for compound Q was obtained, which turned out to have key features in common with the EXAFS structure [14]. For example, a bis- μ -oxo diamond core was obtained with two quite different Fe-O distances, one short at 1.75 Å (exp. 1.77 Å) and one long at 2.03 Å (exp. 2.05 Å). However, the Fe-Fe distance of 2.46 Å given by EXAFS is substantially shorter than the one obtained for the simple model of 2.79 Å. In the second B3LYP study (paper II) [35], a better model including 40–45 atoms was used where the actual histidine ligands were modeled by imidazoles and the glutamates by formates. Systematic attempts to modify the structure were made in order to minimize the Fe-Fe distance. The shortest Fe-Fe distance obtained was 2.54 Å, found for a structure with two bridging carboxylates. Since this structure has four bridges it is difficult to imagine any structure that could have a shorter Fe-Fe distance. Simultaneously, an interesting model dimer was synthesized with two bidentate carboxylate bridges, $\text{Fe}_2(\mu\text{-OH})_2(\mu\text{-O}_2\text{CAr})_2(\text{O}_2\text{CAr})_2(\text{py})_2$, and it was shown that these bridges shortened the Fe-Fe distance by at least 0.2 Å [50]. In another later B3LYP study, a similar structure was suggested for compound Q [36]. As mentioned in the Introduction, Friesner and co-workers [37] recently used a very large iron dimer model including about 100 atoms and suggested a somewhat different structure for compound Q; see Fig. 2. This structure, which has only one bridging carboxylate, has a longer Fe-Fe distance by 0.13 Å compared to the old Q structure in Fig. 2, but was suggested to be 54 kcal/mol more stable. If this huge energy difference would solely be a result of using a larger model, it would clearly cast severe doubts on ever using models where only 40–45 atoms are used for complexes of this type.

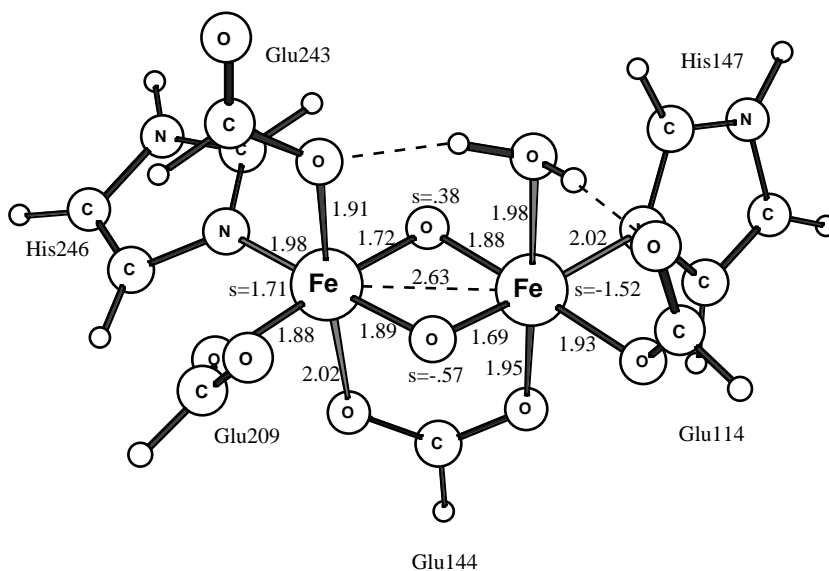
In order to further investigate the origin of the difference between the two Q structures, calculations were performed for the new structure with the small size model. For the old structure a water was added in the second coordination shell, hydrogen bonding between the bridging Glu243 and the terminal Glu114 ligands, in order to make the old and new structures contain the same number of atoms. It was then found that the new structure does indeed have a lower energy than the old one also for the small model. However, the energy difference between the structures is only 9.9 kcal/mol using the small model. The reason this structure was not suggested before was that it was never tried. As mentioned above, the strategy in the

previous study was to try to find the structure with the shortest Fe-Fe distance to get better agreement with EXAFS, and this was obtained with two bridging carboxylates. The Fe-Fe distance is 0.09 Å shorter for the old structure. Even though the Fe-Fe distance thus agrees better with experiment for the old structure, the fact that it is as much as 10 kcal/mol higher in energy makes it a less plausible candidate for compound Q. In the remainder of the present investigation, the new structure is therefore adopted.

A few further comments can be made on the energy difference between the old and new structures for Q. First, a major reason the new structure is better than the old one is that the second sphere water of the new structure is extremely poorly bound. This is consistent with the hydrophobic nature of the active site of MMO. It is therefore probable that the energy difference between the new and old structures could be decreased if the second-sphere water was moved out to the bulk, but probably only by a few kcal/mol. In the study by Friesner and co-workers [37] it was suggested that the additional hydrogen bonding of Glu243 that is opened up for the new structure could be a major reason for the energy difference. To probe the hydrogen bond strength to this carboxylate, a water was therefore added in the second shell, hydrogen bonding to Glu243 of the new structure. The calculated hydrogen bond strength is 7.4 kcal/mol, which is not very strong, again consistent with the hydrophobic nature of the complex. However, part of this hydrogen bond strength could add to the energy difference between the two structures. This appears to be the only additional hydrogen bond to the first-sphere ligands of the complex that is introduced by using the larger model, since no additional second-sphere side chains were introduced. The added atoms are either backbone atoms or atoms connecting the side chains to the backbone. It is therefore difficult to imagine that anything else in the structural model could significantly contribute to the energy difference between the structures. Instead, other differences in the calculations are likely to affect the energy difference. In this context it can be noted that the old structure of Q obtained in the study by Friesner and co-workers has some major differences to the one obtained in the small model. For example, the Fe-Fe distance is much longer: 2.90 Å compared to only 2.54 Å obtained in the small model study at the same level of accuracy.

There is also a notable structural difference in the diamond core between the old Q in the small (40 atom, paper II) model and the new Q of the large (100 atom) model by Friesner and co-workers [37]. In the small, paper II model, two different Fe-O distances were obtained, one to each iron of 1.7 Å and another of 1.9 Å. In the large model by Friesner and co-workers, these distances were found to be much more similar with all four being about 1.80 Å. Two sets of unequal distances were suggested by the first

Fig. 3 Antiferromagnetic $\text{Fe}_2(\text{IV,IV})$ ^1A state of compound Q. Spin populations larger than 0.10 are marked. This structure was optimized with polarization functions on oxygen, unlike the optimizations of all other structures in this study

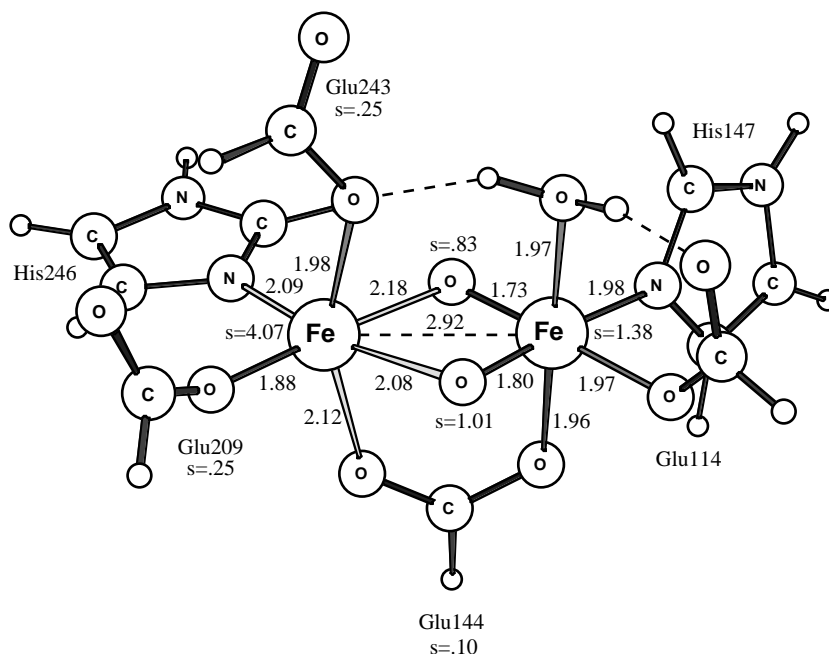


EXAFS study, but in later studies [45, 46, 47, 48, 49] other possible structures were also suggested. Using a small, 40 atom, model for the new Q (where the second sphere water mentioned above has been removed), again two sets of different distances were obtained (see Fig. 3), with one being 1.7 Å and the other one 1.9 Å, in good agreement with the results for the old Q of paper II using the same size model. (Unlike the other structures discussed in the present study, this structure was optimized using a basis set with polarization on the oxygens, since this was found to be of some importance for the Fe-Fe distance.) As mentioned above, the main structural difference between the 40 atom and the 100 atom model should be that there is one more hydrogen bond from the outside to Glu243. However, adding this hydrogen bond has almost no effect on the structure, less than 0.01 Å on the Fe-O distances. The possibility that the other (mostly backbone) atoms added have this effect on the Fe-O distances appears unlikely, since they are without hydrogen bonding to the first sphere, but this remains to be investigated. Another possibility is that different minima were obtained in the two studies. In order to investigate this further, the Fe-O distances were varied, moving one or both of the oxygens between the irons. It was found that the oxygens can quite easily move around in this region from iron to iron at a cost of only a few kcal/mol, and a few local minima were located. The lowest energy of the structures tried for the small model was obtained for the one in the figure. There are two possibilities. One of the studies may have missed the lowest minimum, or the lowest minimum in the two models are actually different. The large flexibility of the diamond core in this type of highly oxidized complexes is supported by recent model studies, where a bridging μ -oxo group was interpreted to isomerize to a terminal oxo group [45, 46, 47, 48, 49].

The present investigation of different compound Q structures has also led to a reinterpretation concerning the spin coupling of the irons. It was already noted in the previous study that antiferromagnetic coupling of the iron spins did not only lead to a substantial shortening of the Fe-Fe bond, but also led to a significant reduction in the size of the individual iron spins, from about 3.0 for the ferromagnetic ^9A state down to 1.5 for the ^1A antiferromagnetic state. Increased experience from modeling these types of complexes has now led to a reconsideration of how this should be interpreted. Rather than a direct effect of antiferromagnetic coupling, it is much more likely that this is simply an effect of low-spin ($S=1$) coupling of the individual irons. This should mean that the true ferromagnetically coupled state corresponding to the antiferromagnetic ^1A state should have a lower spin than 9. An optimization of the structure of the ferromagnetic ^5A state indeed showed that this was the case. The ^5A state turned out to give a geometric structure, energy, and spin distribution that is nearly identical to the ^1A state except for the relative orientations of the spins. The very similar energy (within one kcal/mol) obtained for ferro- and antiferromagnetic coupling is consistent with the low J -value (less than -30 cm^{-1}) estimated from compound Q from Mössbauer spectroscopy [13]. It thus appears from the present results that it is not the antiferromagnetic coupling that is important for shortening the Fe-Fe bond distance, but rather the low-spin ($S=1$) coupling of the individual iron spins.

The freedom to choose the individual spin couplings of the irons in the complex as either high-spin ($S=2$) or low-spin ($S=1$) leads to an additional set of possible spin states, which were investigated. The most interesting of these new structures is the one shown in Fig. 4, with iron spins of 4.07 and 1.38, ferromagnetically coupled. This ^9A structure has an energy which is only 2.3 kcal/mol higher in energy than

Fig. 4 Ferromagnetic $\text{Fe}_2(\text{III},\text{V})$ ^9A state of compound Q. Spin populations larger than 0.10 are marked



the ^1A structure in Fig. 3. While the high-spin coupled iron oxidation state of this complex is clearly III ($S=5/2$), with a characteristic structure and spin, the oxidation state of the other, low-spin coupled iron is less clear. One possibility is to simply consider this as an $\text{Fe}_2(\text{III},\text{V})$ complex. It has a somewhat lower spin than the $\text{Fe}(\text{IV})$ ($S=1$) irons of the ^1A structure and also overall shorter bonds. However, since the spins on the μ -oxo oxygens are very high, 0.83 and 1.01, an assignment as $\text{Fe}_2(\text{III},\text{IV})\text{O}^\cdot$ is also possible, although the oxygen radical is located over two oxygens. This structure turns out to be quite important in both the oxygen activation and in the hydroxylation reaction, to be discussed below. It should be noted in this context that this state is different from the ferromagnetic ^9A state in the previous studies, which can be described as a symmetric $\text{Fe}_2(\text{IV},\text{IV})$ state with two high-spin ($S=2$) irons. In the new model of Q that $\text{Fe}_2(\text{IV},\text{IV})$ state is 6.7 kcal/mol higher in energy than the $\text{Fe}_2(\text{III},\text{V})$ [or $\text{Fe}_2(\text{III},\text{IV})\text{O}^\cdot$] state. In the old Q model this energy difference is rather similar with 6.0 kcal/mol. The reason it was not found in the previous study did therefore not depend on the model but rather that states with low-spin ($S=1$) iron centers were not fully explored. It should be added that these states are very easy to miss without starting with a quite specific idea about the structure.

The vibrational frequencies were computed for the $\text{Fe}_2(\text{IV},\text{IV})$ structure in Fig. 3 and for the $\text{Fe}_2(\text{III},\text{V})$ structure in Fig. 4 to see if these show any clear differences. To make these calculations faster, ammonia ligands were used instead of imidazoles. The highest intensity vibrations involving the bridging oxygens were found at 545 and 669 cm^{-1} for the $\text{Fe}_2(\text{IV},\text{IV})$ structure, while the corresponding frequencies for the $\text{Fe}_2(\text{III},\text{V})$ structure were found at 466 and 625 cm^{-1} .

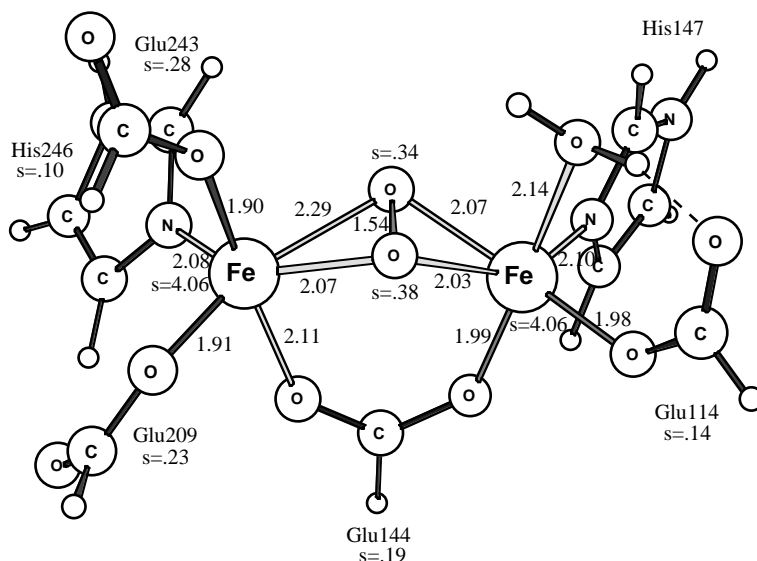
Even though some of these Fe-O bonds are short, they do not appear to give rise to any frequencies in the 850 cm^{-1} region, which has recently been assigned to a terminal Fe=O bond in an iron dimer [45, 46, 47, 48, 49].

The mechanism for O_2 activation

The first part of the MMO reaction sequence is the binding between O_2 and the reduced $\text{Fe}_2(\text{II},\text{II})$ complex, forming the P state. This step will not be studied here, mainly because it has been shown by Friesner and co-workers [37] that very large models (more than a 100 atoms) are needed to describe the loosely bound reduced complex to obtain a reasonable structure and energy. Instead, the first step considered here is the activation of O_2 starting from the P complex. There are a few different reasons to reinvestigate the mechanism for O_2 activation. First, the new structure suggested for Q could alter the mechanism. Second, in the previous study [35], only an approximate transition state was obtained by freezing a reaction coordinate at different distances. Third, an interesting experimental study of the pH dependence of this reaction has recently been presented by Lee and Lipscomb [11]; see the Introduction. In the interpretation of this experiment a heterolytic cleavage of O_2 was suggested, leading to the formation of a water molecule. In the present study, another possible interpretation of the pH dependence is suggested, consistent with a homolytic cleavage, as proposed in the previous B3LYP study.

In line with the new structure for Q, having one glutamate bridge and one water bound to one of the irons, a similar structure was suggested for P by Fries-

Fig. 5 Ferromagnetic $\text{Fe}_2(\text{III,III})$ ^1A state of compound P. Spin populations larger than 0.10 are marked

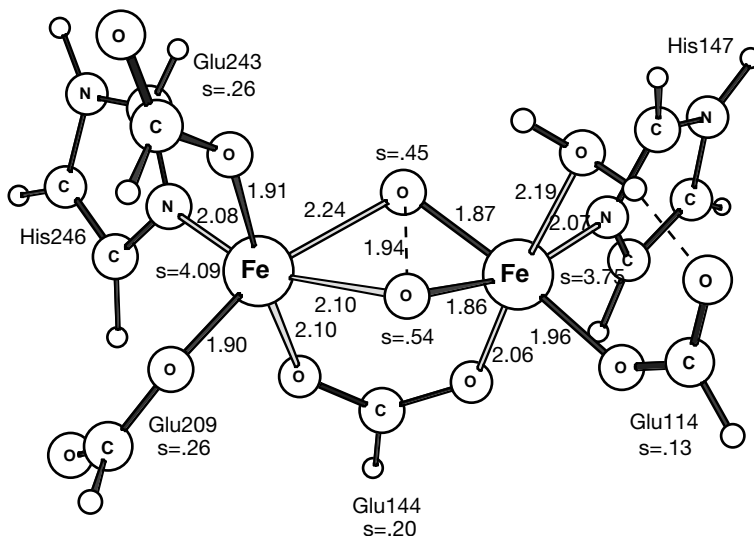


ner and co-workers [37]. In the present study a slightly different structure is suggested, as shown in Fig. 5. This is a rather symmetric $\text{Fe}_2(\text{III,III})$ state, optimized using ferromagnetic coupling (^1A). The irons and O_2 do not lie in a plane, but the oxygens are slightly distorted out from the line connecting the irons. With this position for O_2 the hydrogen bond found in Q between Glu243 on one iron and the water on the other one is broken. It should be noted that the structure of P is very flexible and the presently suggested structure is only the lowest one so far found out of several investigated structures, some of which are quite unsymmetric but which still have very similar energies. An alternative structure for P is therefore certainly possible. The energy for the structure in Fig. 5 is 2.1 kcal/mol more stable than the one found for Q at the same level of treatment. Since, experimentally, Q should be the more stable species, a calculation was performed with two sets of polarization functions on each center, but this actually increased the energy difference to 2.6 kcal/mol. A similar problem was noted in the previous study [35], where P was found to be as much as 8.8 kcal/mol more stable than Q. Part of this problem was rectified by the new more stable structure of Q, but not all of it. In the previous study a slight imbalance in the treatment of different spin states by B3LYP was suggested as a possible origin of the problem. As will be seen below, the situation is more complicated than anticipated.

The homolytic bond cleavage of O_2 in P is an electronically quite complicated process. As the σ -bond of the peroxide is broken an electron should be transferred from iron to the oxygens, which means that one iron should change oxidation state from III to IV. Since the geometric structure of the ligands around Fe(III) is quite different from the one around Fe(IV), the cleavage of O_2 should be closely coupled to a change of many other distances in the complex. To find the transition state is therefore quite difficult and

the attempts in the previous study did not succeed. Instead, an approximate transition state was arrived at by stretching the O-O distance in steps. Based on recent experience, such as with manganese catalase [67], photosystem II (Siegbahn PEM, in preparation), and cytochrome oxidase (Blomberg MRA, Siegbahn PEM, Babcock GT, Wikström M, J Am Chem Soc, submitted), the present attempt to determine a true transition state for the O-O bond cleavage in MMO was successful. The fully optimized transition state is shown in Fig. 6. In this structure, one of the irons remains Fe(III) with spin 4.09 as expected, while the other iron has a spin of 3.75 which is somewhere between the normal spin for Fe(III) and Fe(IV). The Fe-O distance to the Fe(IV) center has decreased markedly from those in P. In the ^1A $\text{Fe}_2(\text{III,IV})$ product of the O-O bond cleavage, the spin on Fe(III) still remains the same, while the spin on Fe(IV) has decreased to its normal high-spin value of 3.11, and the spins on the oxygens have increased to 0.52 and 1.25. This ^1A state is therefore best described as $\text{Fe}_2(\text{III,IV})\text{O}^\cdot$, just like the ^9A state shown in Fig. 4, which is still somewhat different since it has a low-spin ($S=1$) coupling of the Fe(IV) spin. The perhaps most interesting aspect of this mechanism is that essentially only one of the irons is active in the O-O bond-cleavage process. In the final step of the cleavage there should be a few spin-crossings leading from the ^1A $\text{Fe}_2(\text{III,IV})$ state to the antiferromagnetic ^1A $\text{Fe}_2(\text{IV,IV})$ compound Q. Probably, this first occurs by an electron transfer from the inactive Fe(III) to oxygen, leading to high-spin Fe(IV). This iron then crosses to its low-spin ($S=1$) Fe(IV) state and couples antiferromagnetically to the other low-spin ($S=1$) Fe(IV) iron. These spin crossings are expected to be quite efficient since they occur between states with similar geometries and energies in the presence of the large spin-orbit coupling of iron. They were therefore not investigated further. The mechanism of O-O bond

Fig. 6 ^{11}A transition state structure for O-O bond cleavage

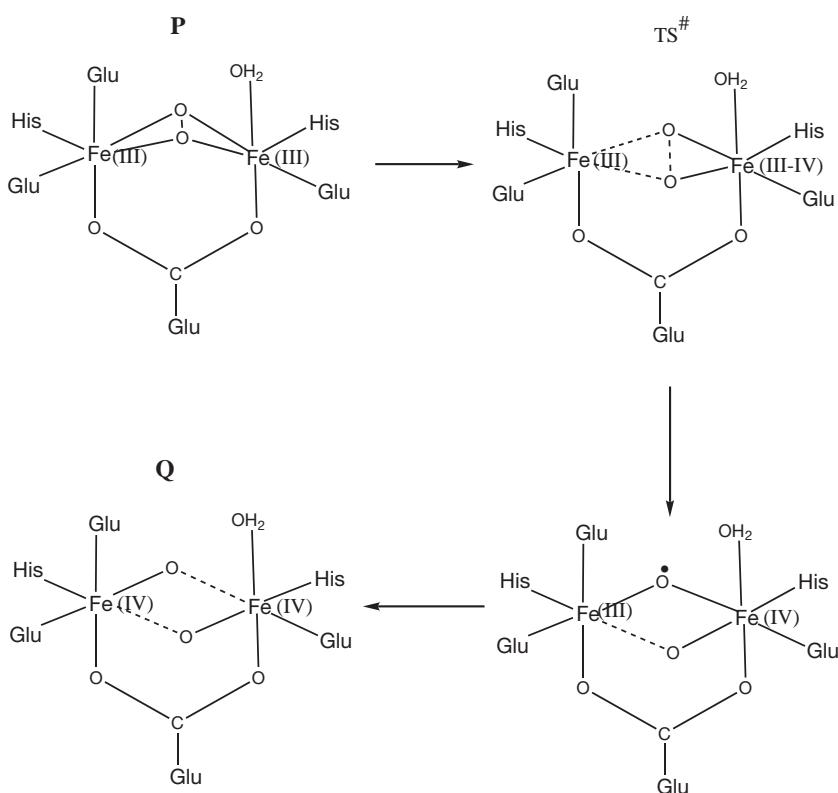


cleavage is shown schematically in Fig. 7. It should be added that this mechanism does not strongly depend on the actual structure of P. Even if P would turn out to be unsymmetrical, the lowest transition state which it has to reach to cleave the O-O bond is still very likely to be the one shown in Fig. 6.

The calculated barrier for O-O bond cleavage is 20.4 kcal/mol, reasonably consistent with the experimental rate of 1 s^{-1} [11], which corresponds to an activation energy of 17 kcal/mol. Still, the homolytic O-O bond cleavage mechanism suggested from both

the previous and the most recent studies is different from the heterolytic one based on experimental studies of the pH dependence [11]; see above. It is therefore of interest to investigate if the measured pH dependence could be rationalized also for a homolytic process. At present, a theoretical study of pH dependence of the present type of reaction is not possible, so more general information has to be used. For this purpose the results from the calculations of the Hessians and from dielectric cavity models could be useful. The temperature dependence obtainable from the Hessians

Fig. 7 Suggested reaction sequence for the O-O bond cleavage of methane



turn out to be quite surprising. The entropy effect in the reaction, normally found to be quite negligible, gives in this case a large effect increasing the endothermicity of the reaction by as much as 8.9 kcal/mol. The reason for this is that the complex significantly decreases in size during the O-O bond cleavage, with a change of the Fe-Fe bond distance from P to Q of almost 1 Å using the present models. This leads to overall increases of the vibrational frequencies including also the smaller ones, important for the entropy, and leads to a smaller entropy for Q than for P. For the same reason, the calculated zero-point vibrational effect on the reaction also increases the endothermicity by 4.3 kcal/mol, which is reduced to 1.9 kcal/mol by temperature-dependent enthalpy effects. It is obvious that in the enzyme a significant change of the size of the system would be strongly limited and the large values calculated for these effects are therefore regarded as artifacts of the model. A proper account of these effects would require not a hundred, but probably thousands of atoms including the entire hydrogen bonding network, which is out of reach at the present stage. A possible, but rather arbitrary, procedure would be to fix certain distances in the model. At present, these effects have simply been estimated to contribute at most a few kcal/mol to the endothermicity of the reaction. It will also be regarded as unnecessary to quantify these effects further if the goal is only to understand the reaction.

With the above estimate of the zero-point and temperature effects of a few kcal/mol, which increases the endothermicity, an effect of at least the same size in the opposite direction becomes necessary to bring the calculated results for the reaction energy in agreement with experiments. A calculation of the dielectric effects using the SCI-PCM method [61, 62] gives no hint of such an effect. However, the optimal size of the system, which is very different for P and Q as discussed above, should also affect the actual strain of the enzyme. There should be considerably less strain for the smaller compound Q than it should be for P, which implies a driving force in the forward direction from strain. The size of this effect, termed the cavitation effect, can be estimated using the DPCM or CPCM methods [63, 64, 65, 66]. If the solvent used is water the strain is estimated to be 5.0 kcal/mol, and if the solvent is diethyl ether it is 4.5 kcal/mol since it has somewhat weaker hydrogen bonds. Using the CPCM method, with a water molecule as a probe and a dielectric constant of 4, gives an effect of 5.4 kcal/mol. The effect on the barrier for O-O bond cleavage is a lowering by 1.2–1.4 kcal/mol due to strain, depending on the method used. For an enzyme the effects could be expected to be somewhat larger than this since the rigidity of the backbone is also involved. It was argued above that the dependence on the size of the complex for the temperature and zero-point effects is an artifact of the model. However, this should not be the case for the cavitation effect, since

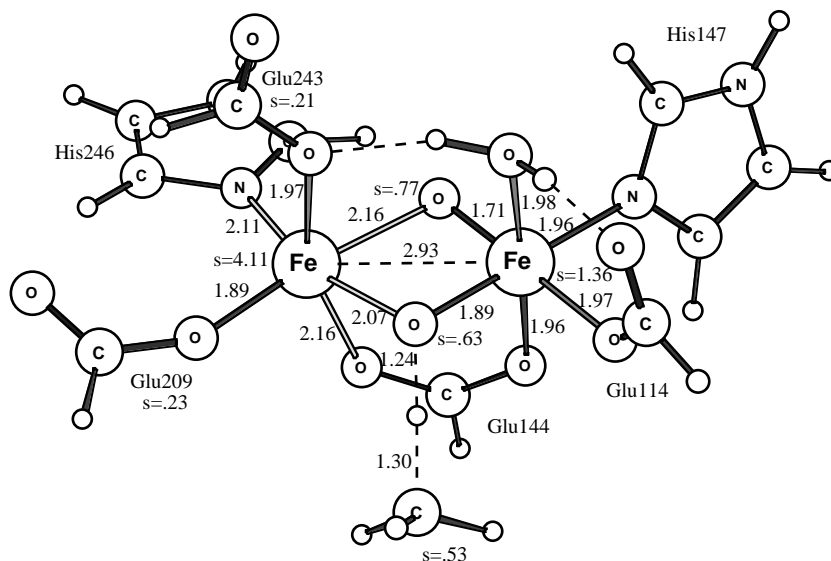
this represents the estimate of the actual strain of the protein. Instead, in a better (and very much larger) model including the protein surroundings, the cavitation effect would be included in the calculated B3LYP energies. Assuming that the protein surroundings would reduce the temperature and zero-point effects to only a few kcal/mol, the cavitation effect could thus correct the present reaction energy to be slightly exothermic.

The above findings concerning the effect of the size of the iron complex can also be used to try to understand the recent experimental results of the pH dependence on the reaction. Since the strain will depend on the strength of the hydrogen bonding network, it is also likely to depend on pH. One possibility is that for lower pH, the additional protons will spread their positive charges, making the hydrogen bonding network stronger, and thus introduce more strain in the system. Another possibility is that the additional protons that appear at lower pH will create entirely new hydrogen bonds that would also increase the strain. Therefore, the best suggestion at present, to make a homolytic cleavage mechanism consistent with the measured pH dependence, is that the increased rate at lower pH is due to a larger cavitation effect. In order to investigate if additional protons have more direct effects on the complex, protons were added at different places on the model complex and the energy difference between P and Q was recomputed. The places tried were the O₂ oxygens and the terminal oxygen of Glu243. However, no such effects leading to a relative stabilization of the product were found. As a final comment, it is also quite difficult to understand how a heterolytic splitting for MMO, in which the protons are supplied from the outside, could occur that would be consistent with the modeling results, with the X-ray structures available, and with the EXAFS results for Q indicating a very short Fe-Fe bond. In the previous model calculations, it was found quite essential for a short Fe-Fe distance that there are two μ -oxo bridges. In practice, this type of heterolytic cleavage would then require that one of the μ -oxo bridges should not come from O₂. A mechanism where a μ -oxo bridge is always present in the complex is not possible either, since it is not present in the X-ray structures of either the reduced or the oxidized forms of MMO. A remaining possibility consistent with a heterolytic splitting is that the protons required are supplied from the ligands of the iron complex. This possibility remains to be investigated.

The mechanism for hydroxylation

The first B3LYP study of MMO (paper I) found a very clean hydrogen abstraction transition state for methane activation [33]. In the second study (paper II), the mechanism was reinvestigated but again the same type of clean transition state was found [35]. In

Fig. 8 ^9A transition state structure (TS1) for C-H activation of methane



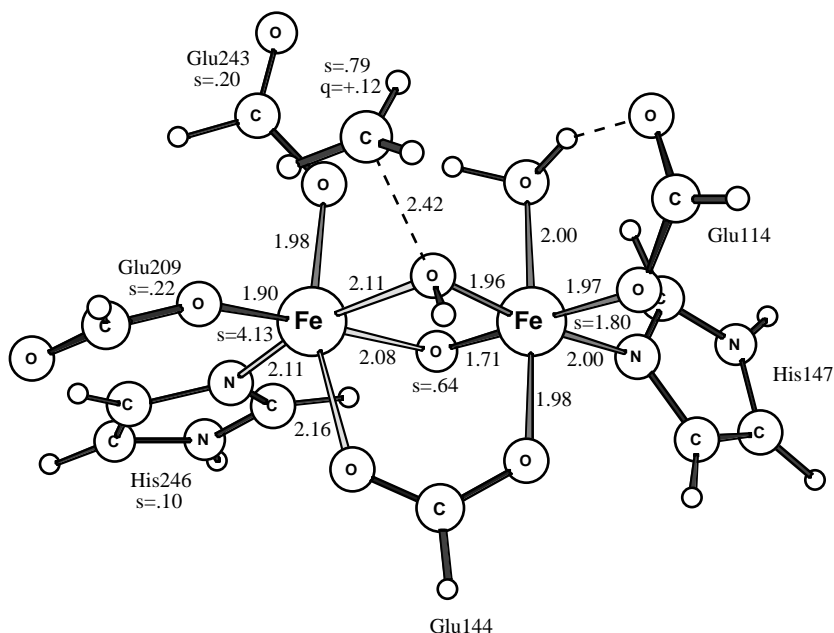
that study, the geometry was also systematically modified to approach a possible insertion transition state by bending the C-H-O angle, but the energy just increased rather steeply. A third study by Basch et al. [36] performed in the meantime also gave the same mechanism. Apart from some studies on rather small and charged models, the results from the theoretical investigations therefore quite conclusively point towards a radical mechanism; see further in the Introduction. It is very unlikely that the use of even larger models is going to change this situation. Still, a few new results will be presented here, where the implications on the mechanism from the finding of the new Q structure in Fig. 3 and the low-lying excited state in Fig. 4 have been investigated.

The presently optimized transition state for C-H activation of methane (TS1) is shown in Fig. 8. This structure differs from the one presented previously mainly by the low-spin ($S=1$) coupling of the Fe(IV) center. The mechanism can be described as starting from a loose complex between methane and the $\text{Fe}_2(\text{III},\text{V})$ structure of Fig. 4 and then abstracting the hydrogen from methane by the bridging oxygen, which initially has a very high spin of 1.01. At the transition state this spin has decreased to 0.63, while the spin on the methyl part has increased from zero to 0.53. The spins on the irons are unchanged at this point. The calculated barrier with respect to Q is 13.8 kcal/mol. The energy for the transition state corresponding to high-spin ($S=2$) [as opposed to low-spin ($S=1$)] coupling of the Fe(IV) center is slightly higher. Overall, the present transition state does not differ significantly from the one presented earlier. The effects of zero-point vibration and temperature on the barrier are in general somewhat problematic, as discussed above for the O_2 bond-cleavage reaction, where a strong artificial dependence of the size of the complex was noted. However, since the transition state and the intermediate $\text{Fe}_2(\text{III},\text{IV})\text{O}\cdot$ complex have about the same size (the optimal Fe-Fe distances are actually almost iden-

tical), these effects should be trusted in the comparison of these systems. The zero-point difference between these systems lowers the barrier by 3.1 kcal/mol. This lowering changes to 4.3 kcal/mol by including also temperature-dependent enthalpy effects. The direction of these effects is expected since the C-H bond, having a large vibrational energy, is broken at the transition state. The entropy effects, on the other hand, increase the barrier by 5.2 kcal/mol, which is also expected since the motion of methane should be nearly free before the reaction (even considering the surrounding enzyme, since no bonds are formed). The effect of strain finally is estimated to lower the barrier by 1.8–2.4 kcal/mol, depending on method used to estimate the strain. Overall, this points towards a barrier counted from $\text{Fe}_2(\text{III},\text{IV})\text{O}\cdot$ of 10 kcal/mol (11.5 kcal/mol without these effects included). It remains to estimate the effects going to this complex from the starting complex Q. The change of zero-point and temperature-dependent enthalpy is -1.4 kcal/mol, of entropy $+3.1$ kcal/mol, and finally the effect of strain is estimated to be $+1.8$ – 2.3 kcal/mol, depending on the method. This means finally that the best estimate of the energy difference between Q and $\text{Fe}_2(\text{III},\text{IV})\text{O}\cdot$ becomes 6 kcal/mol (2.3 kcal/mol without these effects). The barrier going from Q to the transition state should then be 16 kcal/mol (13.8 kcal/mol without these effects). Of the effects added, the ones for zero-point and temperature are most uncertain (see above for the O_2 cleavage reaction), but since these effects only contribute about 2 kcal/mol to the overall barrier, the final estimate of 16 kcal/mol should be reasonable.

Since no significantly new findings were expected for the initial phase of the methane activation, the present study was mainly focused on what happens after the hydrogen abstraction transition state is passed. In the previous study it was assumed, based on pointwise energy calculations, that the reaction would go on to the methyl radical product and then to

Fig. 9 ^9A transition state structure (TS2) for methyl recombination to form methanol

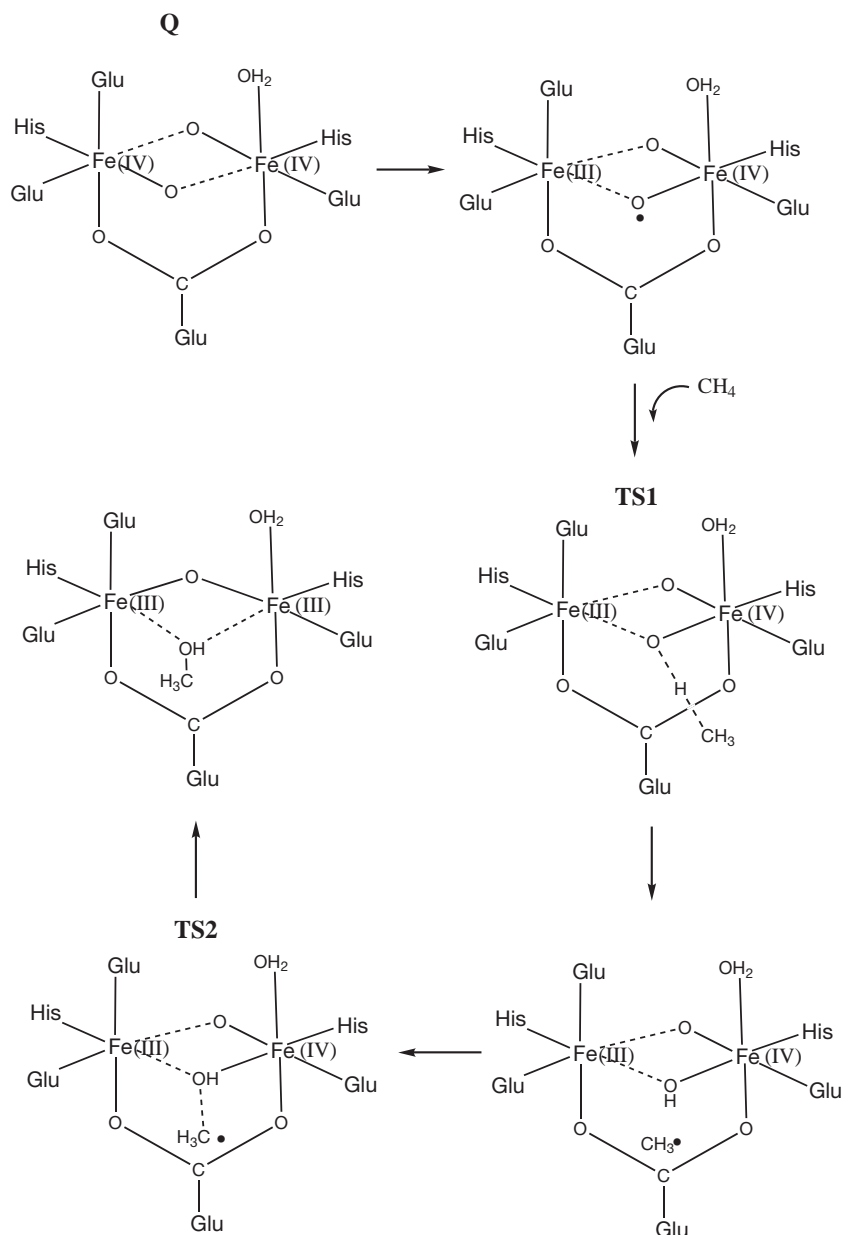


the final methanol product, without any additional barrier. To at least partly rationalize the results of radical clocks, this part of the reaction was assumed to be very fast, mainly because the reaction is very exothermic. However, even with a very fast reaction, it is difficult to see how this mechanism could be consistent with the shortest radical lifetimes estimated experimentally. A search was therefore made to see if there could be a crossing to a potential surface with another spin very shortly after the transition state is passed, in line with suggestions by Shaik and co-workers [51], but no such crossing was found. On the contrary, this search led to still another transition state (TS2), shown in Fig. 9, that had to be passed on the pathway to the products. This type of transition state is the same as had previously been found in the study by Basch et al. [36]. The methanol recombination transition state can be described as one of an electron transfer, much like the one for the activation of O_2 in Fig. 6. For the methanol formation case, the spin on the methyl radical has decreased from 1.0 to 0.79 and there is a corresponding increase on the active low-spin ($S=1$) Fe(IV) center from 1.33 to 1.80. At the end of this reaction step the spin has disappeared from methyl and increased to 2.77 for the active iron, which then has intermediate-spin ($S=3/2$) Fe(III). The spins at the transition state are thus in between those of the reactants and products, which is characteristic of an electron transfer transition state. In the final step of methanol formation, there is a spin crossing where the spin on the active iron center changes from low-spin ($S=3/2$) to high-spin ($S=5/2$) coupling. Another striking similarity to the O_2 reaction is thus that there is essentially only one active iron center in the reaction. The presently suggested hydroxylation mechanism for methane is described schematically in Fig. 10 and the energetics are shown in Fig. 11.

For future modeling purposes the methane hydroxylation reaction was calculated also using ammonia ligands instead of imidazoles. In fact, this model was used throughout the present study to obtain good starting structures for the larger calculations using imidazole ligands. The energies and structures obtained using ammonia ligands were found to be very similar to those for the imidazole model. A similar result was obtained recently also for the catalytic cycle of manganese catalase [67]. In that case the ammonia ligands were not engaged in any hydrogen bonding at all. In the present case, Glu246 becomes artificially hydrogen bonded to the ammonia ligand modeling His246. However, this hydrogen bond stays very much the same throughout the reaction sequence and does therefore not affect the relative energetics significantly. The barrier for O_2 splitting is 20.5 kcal/mol using ammonia and 20.4 kcal/mol using imidazole ligands. The reaction energy of this step differs somewhat more with an exothermicity of 1.8 kcal/mol using ammonia and an endothermicity of 2.1 kcal/mol using imidazole. The methane activation barrier with respect to Q is 14.4 kcal/mol for ammonia and 13.8 kcal/mol for imidazole. Finally, the methanol recombination barrier with respect to the Q starting point is 8.2 kcal/mol for ammonia and 7.6 kcal/mol for imidazole. Apparently, the electronic structure effects from ammonia and imidazole are quite similar. Somewhat larger differences are found when water is used as a model, although the results are still qualitatively the same, which was the motivation for using hydroxyl and water ligands in the first B3LYP study of MMO (paper I) [33].

With the finding of the methanol recombination transition state on the hydroxylation reaction pathway, the deviation to the interpretations of the radical clock experiments is even more definitive than before. To

Fig. 10 Suggested reaction sequence for hydroxylation in methane monooxygenase



rationalize the results of the radical clock experiments, an entirely different explanation therefore has to be found, where an initial formation of an alkyl radical is allowed in spite of the stereochemistry of the products found in these experiments. To approach this difficult problem, some properties of different substrates were investigated. The results are shown in Fig. 12. One critical property of the substrate is clearly the C-H bond strength, which should directly affect the energetics of a hydrogen abstraction. The calculations give results in line with known experiments, with the C-H bond of methane being strongest (102 kcal/mol, calculated), followed by the one of ethane (97 kcal/mol, calculated). For the radical clocks, two C-H bond strengths were evaluated, one leading to the closed (rather unstable) form of the radical and the other one leading to the more stable form, where the cyclo-

propane ring is opened. The C-H bond strength for the closed form (94 kcal/mol) is independent of whether there is a phenyl group attached or not. The phenyl group stabilizes the open form of the radical strongly by resonance effects with 13 kcal/mol and leads to an effective C-H bond strength of only 76 kcal/mol, compared to 89 kcal/mol without the phenyl group. The barrier for rearrangement from the closed to the open form of the radical without the phenyl group was calculated and found to be only 6.2 kcal/mol, also in line with experimental results of 7.5 kcal/mol [68] and theory of 8.5 kcal/mol [69]. These results are fully consistent with the experimental interpretation of the radical clock experiments. In short, if a hydrogen atom is abstracted from the methyl group, the cyclopropane ring should open very quickly, moving the radical site to one of the corners

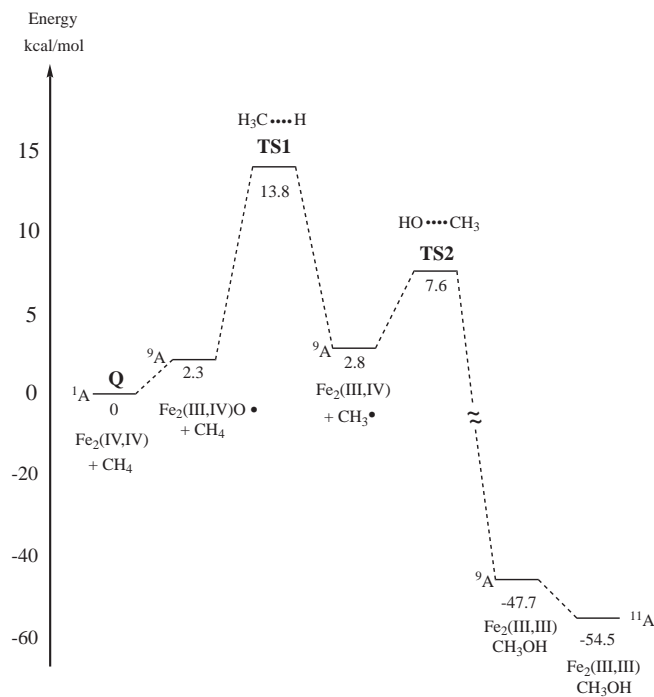


Fig. 11 9A potential energy surface for methanol formation from methane. Note the different scale for the negative y -axis

of the ring. This should lead to hydroxylation at the corner site rather than at the methyl site. Since essentially only hydroxylation at the methyl site is found experimentally, this should mean that no radical with any significant lifetime has formed. It should be added that, at least for the phenyl substituent, where the energy difference between the open and closed forms is 17.4 kcal/mol, the ring opening is irreversible at the time scale of the reaction.

The results for the ionization potentials of the substrates, shown in Fig. 12, are quite interesting and point towards large differences between methane on the one hand and the cyclopropane clocks on the other hand. In particular, the ionization potentials for the radicals differ quite markedly. For methyl it is 229 kcal/mol while for the clocks they are only 151 and 152 kcal/mol. It is clear that this huge difference of 77–78 kcal/mol could have effects on the chemistry, in particular since a very strongly electron-accepting Fe(IV) center is very close by. However, it should be noted that the differences of 77–78 kcal/mol are gas phase differences. The polarizable protein surrounding reduces the difference substantially. For example, using a dielectric constant of 4.0 in the SCI-PCM method leads to a reduction of the difference between the ionization potential of methyl and the unsubstituted clock from 78 kcal/mol to 33 kcal/mol. Since the choice of dielectric constant is somewhat arbitrary, the calculation was rerun with a dielectric constant of 80.0, which should be regarded as an extreme limit. The result is an ionization potential difference of 19 kcal/mol. Still, a rather large difference in ioniza-

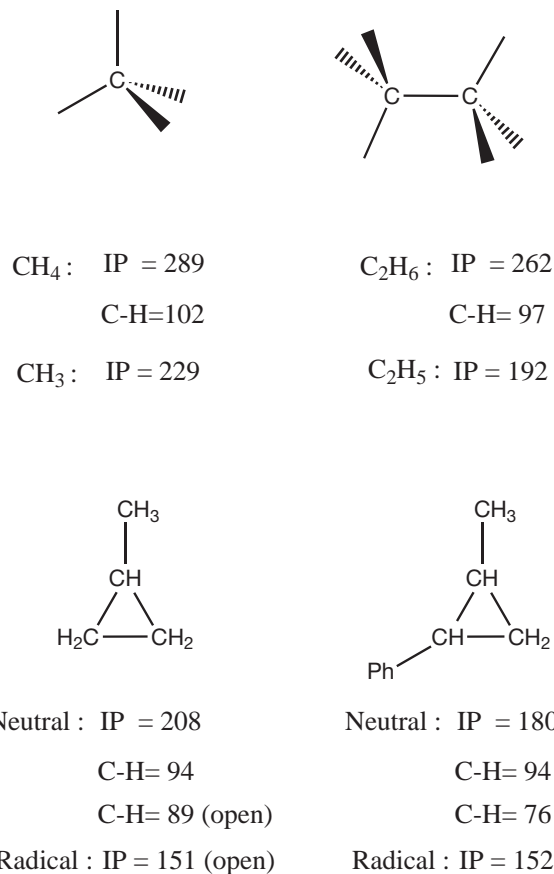
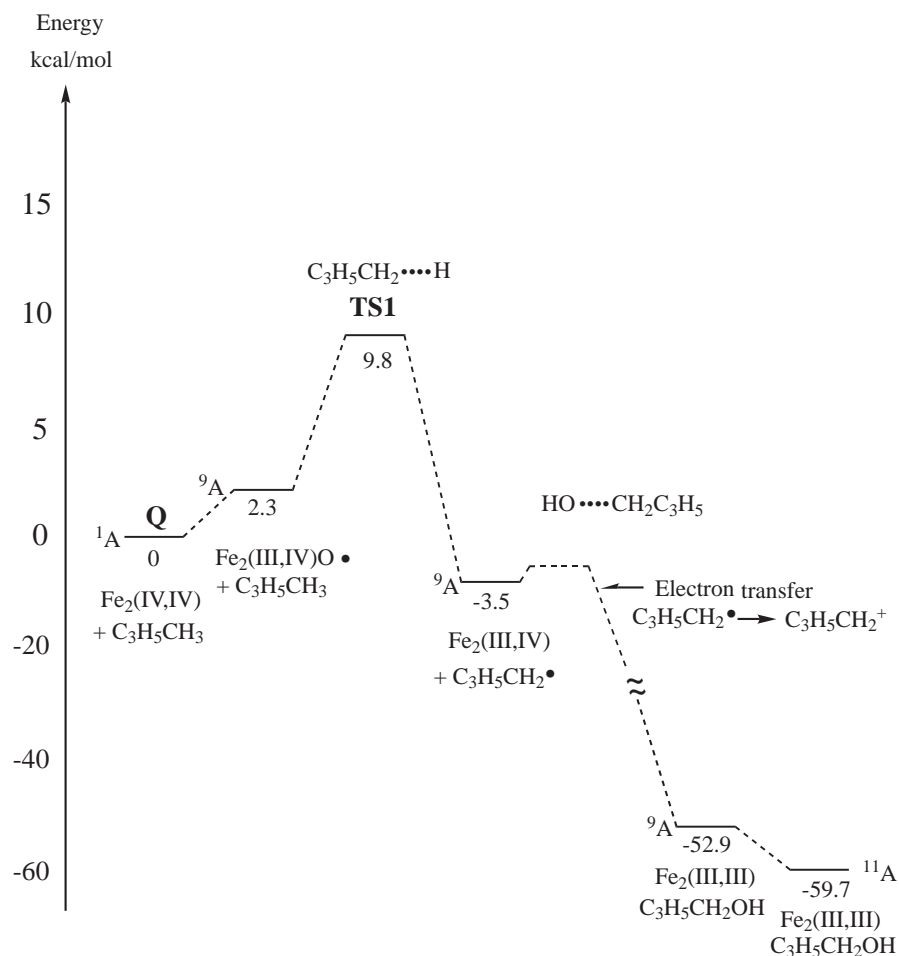


Fig. 12 Calculated ionization potentials and C-H bond strengths (kcal/mol) for different substrates of MMO. For the cyclopropane clock substrates the C-H bond strengths leading to the open structure are marked with *open*. The ionization potentials for the radicals refer to the open form

tion potential between methyl and the radical clock thus persists, which could be decisive for the chemistry. A point worth noting for the cations of the radicals of the clocks is that these, like the neutral clock radicals, also are more stable in the open form of the cyclopropane ring. However, while the phenyl-substituted clock is most stable in the expected Ph-CH-CH₂-CH-CH₂⁺ structure, the unsubstituted clock is only stable in its CH₃-CH-CH-CH₂⁺ form, in which a hydrogen has been transferred between two carbons. In fact, the open form of the unsubstituted clock without a hydrogen transfer, CH₂-CH₂-CH-CH₂⁺, is unstable and goes back to the cyclic form without a barrier. Since ring opening of the cation of the unsubstituted clock therefore also requires a hydrogen transfer, the barrier for ring opening is rather large at 20.3 kcal/mol, while there appears to be no barrier for the phenyl-substituted cation clock. The main resonance structure for the open cation of the phenyl substituted clock is Ph(+) = CH-CH₂-CH=CH₂, while there are two leading resonances for the open cation of the unsubstituted clock, CH₃-CH(+)-CH=CH₂ and CH₃-CH=CH-CH₂(+).

Fig. 15 9A potential energy surface for alcohol formation from the cyclopropane radical clock. Note the different scale for the negative y-axis



number of model calculations are rather limited. However, it can be claimed that the results are at least not inconsistent with the experiments from what is known at present. At first sight, it may appear that the formation of the clock cation does not change the argument behind the interpretation of the radical clock experiments, since the cation also has an open cyclopropane structure (at least for the phenyl-substituted clock). In this context, two major differences between the open radical and the open cation should be pointed out. First, when the open cation becomes hydroxylated at the methyl position, it will automatically close the cyclopropane ring again, which means that the temporary opening of the ring may not be noticed in the experiment. Second, and most importantly, for the cation there is no obvious preference for hydroxylation at the ring positions since there is no spin anywhere. In contrast, for the neutral radical, it is the positioning of the spin in one of the corners of the ring that gives rise to the preferred hydroxylation of this position in the open radical. A key conclusion from the above results is that if the radical becomes ionized at any time before it reaches the hydroxyl, and the calculations leave little doubt that this is the case, then the original motivation behind the interpretation of the radical clock experiments no

longer holds. The results of the experiments will no longer depend on the lifetime of the radical. As an extreme, there could in principle be a very long radical lifetime and this would never be observed on the final structure of the products as long as the radical becomes ionized prior to the recombination with the hydroxyl group. The site of hydroxylation for the cation will most probably depend on the charge distribution, in contrast to the dependence on the spin distribution of the radical. The open cation has a charge of +0.35 on the methyl carbon, +0.15 on the next carbon of the original ring, and +0.29 and +0.21 on the other two carbons of the ring. The site of hydroxylation is not possible to predict from the present calculations, but based on the experimental results it appears that the methyl carbon is strongly preferred. This is probably mainly because this carbon should be closest to the hydroxyl group after the hydrogen abstraction, but also because it has a high charge. It should be noted that, after it is ionized, the substrate is not expected to be freely rotating because of the ionic attraction to the hydroxyl group.

Since the frozen structure for the clock in Fig. 14 is so low in energy, there could be a possibility that the clock would reach this point without going over a hydrogen abstraction transition state. In other words,

there might be a direct insertion transition state, as has been suggested by several workers. However, starting with the structure in the figure, and moving the hydrogen back to the methyl fragment, only led to very high energies. It is therefore concluded that the rate-limiting step is a clean hydrogen abstraction also for the unsubstituted clock. The reason the ionization occurs only after the hydrogen abstraction transition state has been passed is clearly that the ionization potential becomes very much lower after this point. For the unsubstituted clock the gas phase ionization potential decreases by as much as 57 kcal/mol going from the starting clock to the open radical. At the present stage it cannot be ruled out that the phenyl-substituted clock would actually be ionized prior to hydrogen abstraction since it has a considerably lower ionization potential. The gas phase difference to the unsubstituted clock is 28 kcal/mol; see Fig. 12. This might also possibly open up for an insertion pathway in that case. To test this hypothesis would require direct calculations on that substrate, which has not been done.

Of the experimental results, the one for ethane has been most difficult to interpret and two entirely opposite interpretations exist [18, 19]. For this reason, some calculations were also done for ethane as a substrate. Of main interest is to see if the ionization potential of ethane, which is in between those for methane and the clocks (see Fig. 12), makes the ethane reaction more similar to one or the other. An optimization with frozen distances in the region of the alcohol recombination transition state for methane, such as for the one in Fig. 14, led to an electronic structure in line with the clocks rather than with methane. The spin of the ethyl fragment is only 0.02 and the charge +0.66. All attempts to find a solution similar to methane failed. The energy of this structure is 6.0 kcal/mol lower than the one for the ethyl radical starting point. This can be compared to a corresponding energy difference of 8.7 kcal/mol found for the clock (see above), which is actually surprisingly close considering the difference in ionization potentials. Methane is the only substrate for which two solutions could be found. For methane, the frozen cationic structure is 1.0 kcal/mol higher in energy than the radical transition state in Fig. 9. However, even methyl will most probably be ionized before it reaches the hydroxyl group, but only after it has already passed the radical recombination transition state. Since the methyl cation might be expected to strongly polarize its surroundings, the dielectric effects were evaluated for the two methane solutions. This turned out to have a rather small effect on the energy difference, with a relative favoring of the cationic solution by 2 kcal/mol, which means that the methyl cation is quite well solvated already by the presence of the iron dimer complex. It should finally be pointed out that the formation of a substrate cation as described above should not be confused with the question of the final

formation of an alcohol cation. To evaluate the probability for formation of an alcohol cation is beyond present possibilities, but it is expected that even when the substrate radical is ionized the alcohol will be formed as neutral, since the electron never leaves the dimer complex. Even though the experimental findings [20, 21, 22, 23, 24, 25, 26] concern a different cation than the one discussed above, these experiments give some support for the possibility of electron transfer processes in the hydroxylation mechanism.

Conclusions

Many of the key questions concerning alkane hydroxylation by MMO have been addressed in the present study. The main new result is that the hydrocarbon substrate is likely to be ionized sometime prior to the formation of the alcohol. This ionization occurs after a clean hydrogen abstraction transition state has been passed for the substrates studied here. The reason the substrate is ionized after the transition state, rather than before, is that the ionization potential becomes much smaller after this point is passed. The formation of a substrate cation has several important implications for interpretations of experiments on the hydroxylation process. For example, the spin distribution of the substrate radical intermediate is no longer a significant factor for the preferred hydroxylation position of the substrate. Instead, the charge distribution of the cation formed, and the positioning of the substrate with respect to the hydroxyl group after the hydrogen atom has been abstracted, are expected to be more relevant indicators of this preference. The present calculations thus suggest that there is no conflict between the initial formation of a free substrate radical and the hydroxylation products found in radical clock experiments [20, 21, 22, 23, 24, 25, 26]. This explanation is quite different from the one previously given by Shaik and co-workers [51] concerning very similar results for P-450, where a spin crossing was suggested to explain the radical clock experiments. No such spin crossing is found here for MMO, indicating that this should not be an essential factor explaining the outcome of the radical clock experiments. Instead, it is suggested here that the electron transfer from the substrate to the metal complex leading to the formation of a cation, which occurs for MMO, is also an important feature for P-450.

A fully optimized transition state for the activation of the O-O bond of the oxygen molecule by the iron dimer complex has also been obtained for the first time. The transition state is one of a pure homolytic cleavage of the O-O bond. The most interesting result obtained here is that the strain of the enzyme should constitute a significant driving force of about 5 kcal/mol for the bond cleavage process. The reason for this is that without strain the reactant (compound P) is much bigger than the product (compound Q). This is

seen in the present gas phase calculations by the much longer Fe-Fe distance for P. Since the strain of the enzyme should be related to the strength of the hydrogen bonding network, and this strength should be pH dependent, it is speculated here that the recent pH dependence found experimentally for this reaction [11] is related to changes of the strain in the enzyme, rather than a more direct participation of protons in the process.

As described above, the reaction mechanism for hydroxylation of alkanes by MMO is a quite complicated chemical process. The extreme oxidation of the iron dimer complex makes a large number of intermediate states accessible, and therefore also opens up a large number of possible reaction pathways. The DFT studies performed to this date have led to new insights and given new information difficult to obtain by experiments. Undoubtedly, also future theoretical studies will continue to provide new results that will modify the present picture of the mechanism to some extent, and many more studies of this type for MMO can therefore be expected.

Acknowledgements The author is grateful to M. Newcomb and J.D. Lipscomb for valuable discussions and to R.A. Friesner for sending a manuscript prior to publication.

References

- Feig AL, Lippard SJ (1994) *Chem Rev* 94:759–805
- Wallar BJ, Lipscomb JD (1996) *Chem Rev* 96:2625–2657
- Valentine AM, Lippard SJ (1997) *J Chem Soc Dalton Trans* 3925
- Solomon EI, Brunold TC, Davis MI, Kemsley JN, Lee S-K, Lehnert N, Neese F, Skulan AJ, Yang Y-S, Zhou J (2000) *Chem Rev* 100:235–349
- Liu Y, Nesheim JC, Lee SK, Lipscomb JD (1995) *J Biol Chem* 270:24662–24665
- Rosenzweig AC, Nordlund P, Takahara PM, Frederick CA, Lippard SJ (1995) *Chem Biol* 2:409–418
- Rosenzweig AC, Frederick CA, Lippard SJ, Nordlund P (1993) *Nature* 366:537–543
- Elango N, Radhakrishnan R, Froland WA, Wallar BJ, Earhart CA, Lipscomb JD, Ohlendorf DH (1997) *Protein Sci* 6:556–568
- Lippard SJ, Berg J (1994) *Principles of bioinorganic chemistry*. University Science Books, Mill Valley, Calif., p 218
- Orville AM, Lipscomb JD, Ohlendorf DH (1997) *Biochemistry* 36:10052–10066
- Lee S-K, Lipscomb JD (1999) *Biochemistry* 38:4423–4432
- Siegbahn PEM, Blomberg MRA (1999) *Annu Rev Phys Chem* 50:221–249
- Lee S-K, Fox BG, Froland WA, Lipscomb JD, Münck E (1993) *J Am Chem Soc* 115:6450–6451
- Shu L, Nesheim JC, Kauffmann K, Münck E, Lipscomb JD, Que L Jr (1997) *Science* 275:515–518
- Nesheim JC, Lipscomb JD (1996) *Biochemistry* 35:10240–10247
- Lipscomb JD, Que L Jr (1998) *JBIC* 3:331–336
- Deighton N, Podmore ID, Symons MCR, Wilkins PC, Dalton H (1991) *J Chem Soc Chem Commun* 1086–1088
- Priestley ND, Floss HG, Froland WA, Lipscomb JD, Williams PG, Morimoto H (1992) *J Am Chem Soc* 114:7561–7562
- Valentine AM, Wilkinson B, Liu KE, Komarpanicucci S, Priestley ND, Williams PG, Morimoto H, Floss HG, Lippard SJ (1997) *J Am Chem Soc* 119:1818–1827
- Liu KE, Johnson CC, Newcomb M, Lippard SJ (1993) *J Am Chem Soc* 115:939–947
- Choi S-Y, Eaton PE, Hollenberg PF, Liu KE, Lippard SJ, Newcomb M, Putt DA, Upadhyaya SP, Xiong Y (1996) *J Am Chem Soc* 118:6547–6555
- Toy PH, Newcomb M, Hollenberg PF (1998) *J Am Chem Soc* 120:7719–7729
- Toy PH, Newcomb M, Coon MJ, Vaz AD (1998) *J Am Chem Soc* 120:9718–9719
- Whittington DA, Valentine AM, Lippard SJ (1998) *JBIC* 3:307–313
- Valentine AM, Le Tadic-Biadatti M-H, Toy PH, Newcomb M, Lippard SJ (1999) *J Biol Chem* 274:10771–10776
- Newcomb M, Shen R, Choi S-Y, Toy PH, Hollenberg PF, Vaz AD, Coon MJ (2000) *J Am Chem Soc* 121:2677–2686
- Ruzicka F, Huang DS, Donnelly MI, Frey PA (1990) *Biochemistry* 29:1696–1700
- Jin Y, Lipscomb JD (1999) *Biochemistry* 38:6178–6186
- Choi S-Y, Eaton PE, Kopp DA, Lippard SJ, Newcomb M, Shen R (1999) *J Am Chem Soc* 121:12198–12199
- Sono M, Roach MP, Coulter ED, Dawson JH (1996) *Chem Rev* 96:2841–2887
- Blomberg MRA, Siegbahn PEM, Babcock GT, Wikström M (2000) *J Inorg Biochem* 80:261–269
- Wirstam M, Blomberg MRA, Siegbahn PEM (1999) *J Am Chem Soc* 121:10178–10185
- Siegbahn PEM, Crabtree RH (1997) *J Am Chem Soc* 119:3103–3113
- Siegbahn PEM, Crabtree RH, Nordlund P (1998) *JBIC* 3:314–317
- Siegbahn PEM (1999) *Inorg Chem* 38:2880–2889
- Basch H, Mogi K, Musaev DG, Morokuma K (1999) *J Am Chem Soc* 121:7249–7256
- Dunietz BD, Beachy MD, Cao Y, Whittington DA, Lippard SJ, Friesner RA (2000) *J Am Chem Soc* 122:2828–2839
- Yoshizawa K (1998) *JBIC* 3:318–324
- Yoshizawa K, Shiota Y, Yamabe T (1998) *Organometallics* 17:2825–2831
- Yoshizawa K, Ohta T, Shiota Y, Yamabe T (1997) *Chem Lett* 1213–1214
- Yoshizawa K, Ohta T, Shiota Y, Yamabe T (1998) *Bull Chem Soc Jpn* 71:1899
- Yoshizawa K, Suzuki A, Shiota Y, Yamabe T (2000) *Bull Chem Soc Jpn* 73:815–827
- Shestakov AF, Shilov AE (1996) *J Mol Catal A* 105:1–7
- Burdi D, Willems J-P, Riggs-Gelasco P, Antholine WE, Stubbe J, Hoffman BM (1998) *J Am Chem Soc* 120:12910–12919
- Que L Jr (1997) *J Chem Soc Dalton Trans* 3933–3940
- Hsu HF, Dong Y, Shu L, Young VG Jr, Que L Jr (1999) *J Am Chem Soc* 121:5230–5237
- Dong Y, Fujii H, Hendrich MP, Leising RA, Pan G, Randall CR, Wilkinson EC, Zang Y, Que L Jr, Fox BG, Kauffman K, Münck E (1995) *J Am Chem Soc* 117:2778–2792
- Dong Y, Que L Jr, Kauffman K, Münck E (1995) *J Am Chem Soc* 117:11377–11378
- Dong Y, Zang Y, Shu L, Wilkinson EC, Kauffman K, Münck E, Que L Jr (1997) *J Am Chem Soc* 119:12683–12684
- Lee D, Lippard SJ (1998) *J Am Chem Soc* 120:12153–12154
- Filatov M, Harris N, Shaik S (1999) *Angew Chem Int Ed* 38:3510–3512
- Becke AD (1998) *Phys Rev A* 38:3098
- Becke AD (1993) *J Chem Phys* 98:1372
- Becke AD (1993) *J Chem Phys* 98:5648
- Stevens PJ, Devlin FJ, Chablowski CF, Frisch MJ (1994) *J Phys Chem* 98:11623

56. Frisch MJ, Trucks GW, Schlegel HB, Gill PMW, Johnson BG, Robb MA, Cheeseman JR, Keith T, Petersson GA, Montgomery JA, Raghavachari K, Al-Laham MA, Zakrzewski VG, Ortiz JV, Foresman JB, Cioslowski J, Stefanov BB, Nanayakkara A, Challacombe M, Peng CY, Ayala PY, Chen W, Wong MW, Andres JL, Replogle ES, Gomperts R, Martin RL, Fox DJ, Binkley JS, Defrees DJ, Baker J, Stewart JP, Head-Gordon M, Gonzalez C, Pople JA (1995) Gaussian 94, revision B.2. Gaussian, Pittsburgh
57. Frisch MJ, Trucks GW, Schlegel HB, Scuseria GE, Robb MA, Cheeseman JR, Zakrzewski VG, Montgomery JA Jr, Stratmann RE, Burant JC, Dapprich S, Millan JM, Daniels AD, Kudin KN, Strain MC, Farkas O, Tomasi J, Barone V, Cossi M, Cammi R, Mennucci B, Pomelli C, Adamo C, Clifford S, Ochterski J, Petersson GA, Ayala PY, Cui Q, Morokuma K, Malick DK, Rabuck AD, Raghavachari K, Foresman JB, Cioslowski J, Ortiz JV, Stefanov BB, Liu G, Liashenko A, Piskorz P, Komaromi I, Gomperts R, Martin RL, Fox DJ, Keith T, Al-Laham MA, Peng CY, Nanayakkara A, Gonzalez C, Challacombe M, Gill PMW, Johnson B, Chen W, Wong MW, Andres JL, Head-Gordon M, Replogle ES, Pople JA (1998) Gaussian 98. Gaussian, Pittsburgh
58. Hay PJ, Wadt WR (1985) *J Chem Phys* 82:299
59. Bauschlicher CW Jr, Ricca A, Partridge H, Langhoff SR (1997) In: Chong DP (ed) *Recent advances in density functional methods, part II*. World Scientific, Singapore, p 165
60. Siegbahn PEM (1996) *Adv Chem Phys* 93:333
61. Wiberg KB, Rablen PR, Rush DJ, Keith TA (1995) *J Am Chem Soc* 117:4261
62. Wiberg KB, Keith TA, Frisch MJ, Murcko M (1995) *J Phys Chem* 99:9072
63. Miertus S, Scrocco E, Tomasi J (1981) *Chem Phys* 114:117
64. Miertus S, Tomasi J (1982) *Chem Phys* 65:239
65. Cossi M, Barone V, Cammi R, Tomasi J (1996) *Chem Phys Lett* 255:327
66. Barone V, Cossi M (1998) *J Phys Chem* 102:1995–2001
67. Siegbahn PEM (2000) *Theor Chem Acc* (in press)
68. Newcomb M, Glenn AG (1989) *J Am Chem Soc* 111:275–277
69. Smith DM, Nicolaides A, Golding BT, Radom L (1998) *J Am Chem Soc* 120:10223–10233